Current Optics and Photonics
Vol. 1, No. 2, April 2017, pp. 138-142

ISSN: 2508-7266(Print) / ISSN: 2508-7274(Online)
DOI: https://doi.org/10.3807/COPP.2017.1.2.138

Terahertz Generation Based on Cascaded Difference Frequency Generation with Periodically-poled $KTiOPO_4$

Zhongyang Li*, Silei Wang, Mengtao Wang, and Weishu Wang

North China University of Water Resources and Electric Power, 36, Bei-huan Road, Zhengzhou, Henan, 450045, P. R. China

(Received May 31, 2016 : revised November 12, 2016 : accepted March 8, 2017)

Terahertz (THz) generation by periodically-poled $KTiOPO_4$ (PPKTP) with a quasi-phase-matching scheme based on cascaded difference frequency generation (DFG) processes is theoretically analyzed. The cascaded Stokes interaction processes and the cascaded anti-Stokes interaction processes are investigated from coupled wave equations. THz intensities and quantum conversion efficiency are calculated. Compared with non-cascaded DFG processes, THz intensities from 10-order cascaded DFG processes are increased to 5.53. The quantum conversion efficiency of 479.4% in cascaded processes, which exceeds the Manley-Rowe limit, can be realized.

Keywords : Terahertz wave; Cascaded difference frequency generation; $KTiOPO_4$
OCIS codes : (190.4410) Nonlinear optics, parametric process; (140.3070) Infrared and far-infrared lasers

I. INTRODUCTION

The terahertz (THz) radiation, which generally is considered to comprise the frequency from 0.1 to 10 THz, has recently drawn much attention due to its tremendous potential applications, such as imaging, material detection, environmental monitoring, communication, astronomy and national defense security [1-4]. For such applications, a high-power, widely tunable, and compact source of THz waves is required. Among many electronic and optical methods for coherent THz wave generation, difference frequency generation (DFG) [5-8] is of importance because it offers the advantages of relative compactness, narrow linewidth, wide tuning range, high power output and room temperature working environment. Unfortunately, the quantum conversion efficiency of the DFG is extremely low as the THz wave is intensely absorbed by the nonlinear optical crystal. To improve the low quantum conversion efficiency and overcome the Manley-Rowe limit, cascaded DFG in which more than one THz photon is generated from the depletion of a single pump photon is a promising method. Theoretical descriptions and experimental demonstrations of an enhancement output of THz wave via cascaded DFG processes have been reported recently [9-11].

$KTiOPO_4$ (KTP) crystal is an attractive material for the nonlinear optical interaction between optical and THz waves due to its wide transmission range (0.35-4.5 μm) [12], a relatively high nonlinear coefficient (d_{33}=15.4 pm/V at 1064nm) [13] and a high optical damage threshold of 10 J/cm^2 at 1064 nm [14]. KTP crystal has been widely studied and applied in THz generation based on stimulated polariton scattering (SPS) processes [15-17]. Compared with lithium niobate ($LiNbO_3$) and lithium tantalate ($LiTaO_3$) in THz generation based on optical parametric mixing, KTP is known to have a higher laser damage threshold. Moreover, the refractive indices of KTP in the THz range are about 20% lower than that of $LiNbO_3$ [18, 19], providing a high figure of merit and enabling a better outcoupling of the THz radiation from the crystals. Compared with zinc-blende structure materials in THz generation based on DFG, such as GaAs, InP, ZnTe and GaP, KTP has a high laser damage threshold, and it is relatively inexpensive.

In this paper, we present the theoretical analysis of THz generation by periodically-poled KTP (PPKTP) with a

*Corresponding author: thzwave@163.com
Color versions of one or more of the figures in this paper are available online.

quasi-phase-matching scheme based on cascaded DFG processes. We investigate the cascaded Stokes interaction processes and the cascaded anti-Stokes interaction processes. THz intensities and quantum conversion efficiency are calculated from coupled wave equations.

II. THEORETICAL MODEL

Figure 1 shows a schematic diagram of THz wave generation by quasi-phase-matching cascaded DFG. Pump (ω_p) and signal (ω_s) waves propagate along the x axis of the PPKTP crystal, and a THz wave (ω_T) is generated by forward parametric processes when both of the electric field of pump and signal waves are along the z-axis of the KTP crystal. A THz wave is generated via interactions between the incident pump and signal waves in the first-order DFG process, which consumes the higher frequency pump photon and amplifies the lower frequency signal photon. The amplified signal wave also acts as a higher frequency pump wave, which amplifies the THz wave and generates a new lower frequency cascaded signal (ω_{cs}) wave in the second-order DFG process. Simultaneously, anti-Stokes interactions will also occur that consume the THz photon and pump photon, resulting in a higher frequency anti-Stokes signal (ω_{cp}) wave. The cascaded Stokes processes and anti-Stokes processes can be continued to any high order as long as the phase-matching conditions are satisfied. The intensity of the THz wave is determined by a trade-off between the Stokes processes and the anti-Stokes processes.

The coupled wave equations of cascaded DFG can be derived from common nonlinear optical three-wave interaction equations, shown as

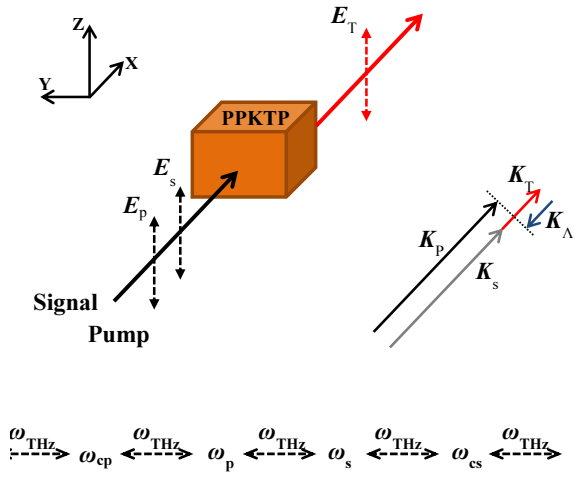

FIG. 1. Schematic diagram of the cascaded DFG to generate THz radiation by PPKTP crystal. The electric field vectors of pump E_p, signal E_s and THz E_T are all along the z-axis of KTP crystal. The wave vectors of pump K_p, signal K_s, THz K_T, and K_Λ satisfy the forward parametric processes.

$$\frac{dE_T}{dz} = -\frac{\alpha_T}{2}E_T + \kappa_T \sum_1^{+\infty} E_n E_{n+1}\, cos(\Delta k_n z) \tag{1}$$

$$\frac{dE_n}{dz} = -\frac{\alpha_n}{2}E_n + \kappa_n E_{n-1} E_T cos(\Delta k_{n-1} z) - \kappa_n E_{n+1} E_T cos(\Delta k_n z) \tag{2}$$

$$\kappa_n = \frac{\omega_n d_{eff}}{c n_n} \tag{3}$$

$$\kappa_T = \frac{\omega_T d_{eff}}{c n_{T.eff}} \tag{4}$$

$$\Delta k_n = k_n - k_{n+1} - k_T + \frac{2\pi}{\Lambda} \tag{5}$$

$$\omega_T = \omega_n - \omega_{n-1} \tag{6}$$

$$I = \frac{1}{2} n_n c \varepsilon_0 |E|^2 \tag{7}$$

where ω_n and ω_T denote the frequency of pump and THz wave, respectively. E_n and E_T denote the electric field amplitude of pump and THz wave, respectively. α_n and α_T denote the absorption coefficient of pump and THz wave in the optical crystal, respectively. Δk_n indicates the wave vector mismatch in the cascaded DFG process, k_n and k_T are the coupling coefficients. d_{eff} is the effective nonlinear coefficient. c is the speed of light in vacuum, ϵ_0 is the vacuum dielectric constant, I is the power density, n_n is the refractive index and Λ is the poling period of PPKTP. The generation and consumption of THz photons are accomplished during the interaction between the n-order and (n+1)-order Stokes waves, as shown in Eq. (1). The second item to the right of the equal sign in Eq. (2) shows the Stokes processes where THz photons and n-order Stokes photons are generated, and the third item to the right of the equal sign in Eq. (2) shows the anti-Stokes processes where THz photons and (n+1)-order Stokes photons are consumed. The theoretical values of refractive index are calculated using a wavelength-independent Sellmeier equation for KTP in the infrared [20] and THz [19] ranges, respectively.

III. CALCULATIONS

Here, in simulating the cascaded DFG dynamics, pump wave ω_p and signal wave ω_s are supposed to be 282 and 281 THz, respectively. THz frequency ω_T is taken to be 1 THz. The wave vector mismatch Δk and coherence length in cascaded DFG processes is shown in Fig. 2. According to the Eq. (5), the poling period of PPKTP is 205.31 μm to satisfy the first-order Stokes quasi-phase-matching condition.

In the cascaded Stokes processes, wave vector mismatch is less than 3.14 cm^{-1} during a 55-order cascaded process. In the case of cascaded anti-Stokes processes, wave vector mismatch is less than 3.14 cm^{-1} during a 40-order cascaded process. As shown in Fig. 3, THz intensities in PPKTP based on cascaded DFG with cascading orders 1, 3, 5, 7 and 10 versus crystal length are calculated according to Eqs. (1) and (2). The intensities of both pump and signal waves are 10 MW/mm^2. The absorption coefficients at 1 THz is 1.69 cm^{-1}[19]. From the Fig. 3 we find that THz intensities without cascading processes are extremely low. THz intensities with cascading order 3, 5, 7 and 10 are enhanced. THz intensity of 0.102 MW/mm^2 can be obtained with 10-order cascaded Stokes processes. Compared with non-cascaded DFG processes, THz intensities from 10-order cascaded DFG processes are increased to 5.53. In a non-cascaded DFG process, at best, a single THz photon is generated from each pump photon. The cascaded processes can enhance the THz output, simply by generating several THz photons from each pump photon.

Both the influence of wave vector mismatch and absorption has been taken into account in the previous calculations. The comparison of THz wave intensity in three different situations in 10-order cascading processes is described in Fig. 4. The original pump and signal intensities are 10 MW/mm^2 and their frequencies are 282 THz and 281 THz, respectively. As it shows, without absorption and mismatch, the power of the THz wave increases rapidly with propagation distance. Conversely, the maximum intensities of THz radiation obtained are far less as a result of the influence of absorption and wave vector mismatch in the cascaded DFG process. Additionally, it should be noted that higher THz intensity can be obtained considering absorption and no wave vector mismatch.

As the Stokes processes generate a THz photon and the anti-Stokes processes consume a THz photon, THz intensities depend on the Stokes processes and the anti-Stokes processes. Figure 5 shows the maximum intensities of the optical waves during the cascaded Stokes processes and anti-Stokes processes. In this figure we assume that the optical waves at interval of 1 THz with frequencies from 267 to 282 THz interact in the Stokes and anti-Stokes processes. The initial pump and signal waves are 275 and 274 THz with a power density of 10 MW/mm^2, respectively. From the figure we find that the power densities of optical waves in the Stokes processes is higher than that of optical waves in the anti-Stokes processes, which indicates that the Stokes processes are stronger than the anti-Stokes processes. In the cascaded Stokes processes, *n*-order Stokes photons

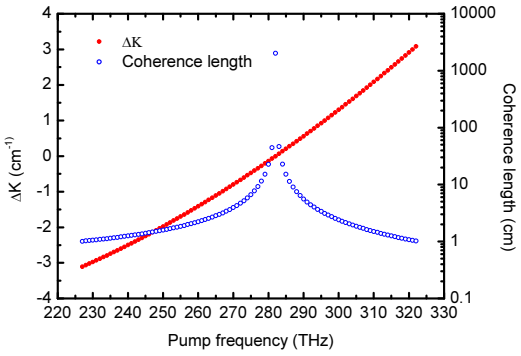

FIG. 2. Wave vector mismatch and coherence length of cascaded DFG. Assuming $\omega_p = 282\,\mathrm{THz}$, $\omega_s = 281\,\mathrm{THz}$, $\omega_T = 1.0\,\mathrm{THz}$.

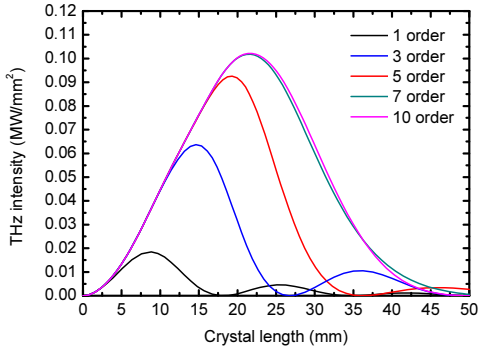

FIG. 3. THz intensities in PPKTP based on cascaded DFG with cascading orders 1, 3, 5, 7 and 10. Assuming $\omega_p = 282\,\mathrm{THz}$, $\omega_s = 281\,\mathrm{THz}$, $\omega_T = 1.0\,\mathrm{THz}$.

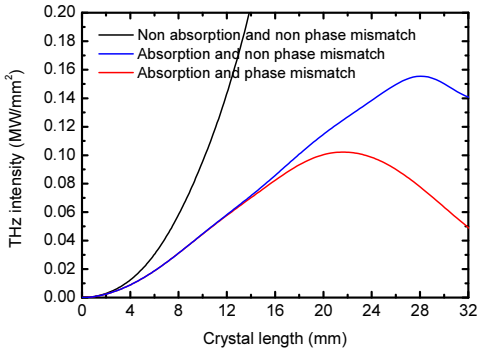

FIG. 4. Influence of absorption and/or wave vector mismatch on generated THz intensity in 10-order cascading processes.

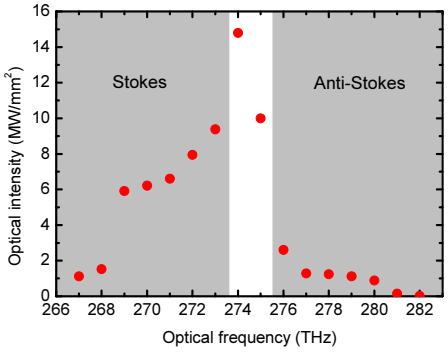

FIG. 5. The maximum intensity of the optical waves during the cascaded Stokes processes and anti-Stokes processes. Assuming the initial pump and signal waves are 275 THz and 274 THz with a power density of 10 MW/mm^2, respectively.

are consumed and (n+1)-order Stokes and THz photons are amplified. The cascaded Stokes processes continue to amplify the (n+1)-order Stokes and THz photons as long as the phase-matching conditions are satisfied. Actually, the anti-Stokes processes take place only if the Stokes processes generate THz photons. The anti-Stokes processes consume high-order Stokes and THz photons, and the processes will stop if the high-order Stokes and THz photons are exhausted.

Figure 6 shows the relationship between the maximum THz intensities and pump wave frequencies. In this figure we assume that the optical waves at interval of 1 THz with frequencies from 267 to 282 THz interact in the cascaded Stokes and anti-Stokes processes. The frequency of pump wave is 1 THz larger than that of the signal wave. Both the pump and signal intensities are 10 MW/mm^2. From the figure we find that THz intensities are higher as the pump frequencies locate in the high-frequency area. The high THz intensities originate from the interaction of the high-order Stokes processes as the pump frequencies locate in the high-frequency area, which indicates that the Stokes processes are stronger than the anti-Stokes processes. In the high-frequency area where high-order Stokes processes

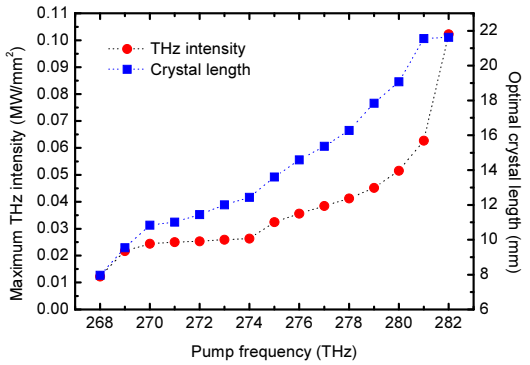

FIG. 6. The relationship between the maximum THz intensities and pump frequencies. Both of the pump and signal intensity are 10 MW/mm^2.

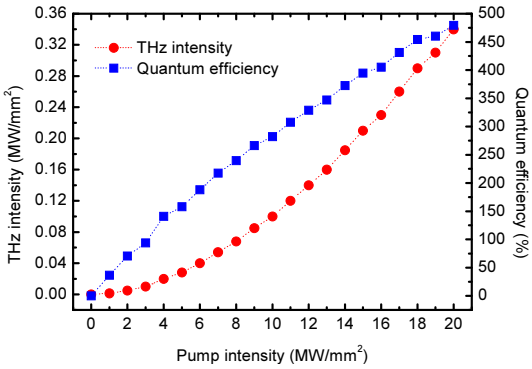

FIG. 7. The maximum THz intensity and quantum conversion efficiency versus pump intensity in 10-order cascading processes. Assuming pump and signal frequencies are 282 and 281 THz, respectively.

interact, optimal crystal lengths are longer considering cascading, which is consistent with the principle of cascaded nonlinear processes.

Pump intensity is directly related to the quantum conversion efficiency in the cascaded DFG processes. The maximum THz intensity and quantum conversion efficiency are calculated during a 10-order cascading processes when the original pump intensities are changed from 0 to 20 MW/mm^2, as shown in Fig. 7. In the calculations, pump wave and signal wave are supposed to be 282 and 281 THz, respectively. Figure 7 demonstrates that the maximum THz intensity and quantum conversion efficiency significantly increase with the pump intensity. THz wave with a maximum intensity of 0.34 MW/mm^2 can be generated at pump intensity equal to 20 MW/mm^2, corresponding to the quantum conversion efficiency of 479.4%. The quantum conversion efficiency of 479.4% in cascaded processes exceeds the Manley-Rowe limit. There are two factors contributing to the high THz intensity and quantum conversion efficiency. Firstly, cascaded DFG processes in which more than one THz photon is generated from the depletion of a single pump photon enhance the output of the THz wave. Secondly, the quasi-phase-matching scheme provides large interaction volume among the three mixing waves. Despite the fact that the THz wave is intensely absorbed by KTP, the non-depletion pump wave and fast growth of the non-absorbing signal wave can assist the growth of the THz wave.

THz generation with the frequency of 1 THz with a quasi-phase-matching scheme based on cascaded DFG processes is theoretically analyzed above. As for THz waves with frequencies lower than 1 THz, THz generation can be effectively enhanced based on cascaded DFG processes if the quasi-phase-matching scheme is satisfied. As for THz wave with frequencies larger than several THz, the output of the THz wave is seriously affected by the absorption by the KTP crystal as the absorption coefficients of the THz wave in KTP crystal rapidly increase with the increase of frequency.

In comparison with THz generations from GaAs and GaP, the intensities of a THz wave at 1 THz generated by cascaded DFG from GaAs and GaP at a pump intensity of 20 MW/mm^2 are 0.62 MW/mm^2 and 0.23 MW/mm^2, respectively [21]. The generated THz intensity and quantum efficiency from KTP are comparable with those from GaAs and GaP.

It is worth noting that parasitic emissions, such as green light and blue light, are simultaneously generated in the processes of THz generations. The parasitic emissions are generated by frequency-doubling and optical parametric oscillation from the PPKTP. The quasi-phase-matching scheme for the pump, signal and THz waves, as shown in Fig. 1, will bring large phase mismatch in the processes of frequency-doubling and optical parametric oscillation. The parasitic emissions propagate noncollinearly with the pump or signal waves, which means that the intensities of the

parasitic emissions are weak. The parasitic emissions which consume the pump photons should be restricted in the experimental design.

IV. CONCLUSION

THz generation by PPKTP with a quasi-phase-matching scheme based on cascaded DFG processes is theoretical analyzed. The cascaded DFG processes comprise the Stokes interaction processes and the cascaded anti-Stokes interaction processes. The calculation results indicate that the Stokes processes are stronger than the anti-Stokes processes. Compared with non-cascaded DFG processes, THz intensities from 10-order cascaded DFG processes are increased to 5.53. A THz wave with a maximum intensity of 0.34 MW/mm^2 can be generated when pump intensity is 20 MW/mm^2, corresponding to the quantum conversion efficiency of 479.4%. The quantum conversion efficiency of 479.4% exceeds the Manley-Rowe limit, which provides us an efficient way to enhance the output of THz waves.

ACKNOWLEDGMENT

This work was supported by the National Natural Science Foundation of China (Grant Nos. 61201101 and 61205003), Young Backbone Teachers in University of Henan Province (Grant No. 2014GGJS-065), Foundation and Advanced Technology Research Program of Henan Province (Grant No. 162300410269), Program for Innovative Research Team (in Science and Technology) in University of Henan Province (Grant No. 16IRTSTHN017).

REFERENCES

1. S. Koenig, D. Lopez-Diaz, J. Antes, F. Boes, R. Henneberger, A. Leuther, A. Tessmann, R. Schmogrow, D. Hillerkuss, R. Palmer, T. Zwick, C. Koos, W. Freude, O. Ambacher, J. Leuthold, and I. Kallfass, "Wireless sub-THz communication system with high data rate," Nat. Photon. **7**, 977-981 (2013).
2. C. M. Watts, D. Shrekenhamer, J. Montoya, G. Lipworth, J. Hunt, T. Sleasman, S. Krishna, D. R. Smith, and W. J. Padilla, "Terahertz compressive imaging with metamaterial spatial light modulators," Nat. Photon. **8**, 605-609 (2014).
3. M. Johnston, "Plasmonics: Superfocusing of terahertz waves," Nat. Photon. **1**, 14-15 (2007).
4. M. Tonouchi, "Cutting-edge terahertz technology," Nat. Photon. **1**, 97-105 (2007).
5. Y. J. Ding, "Progress in terahertz sources based on difference-frequency generation [Invited]," J. Opt. Soc. Am. B **31**, 2696-2711 (2014).
6. A. Majkić, M. Zgonik, A. Petelin, M. Jazbinšek, B. Ruiz, C. Medrano, and P. Günter, "Terahertz source at 9.4 THz based on a dual-wavelength infrared laser and quasi-phase matching in organic crystals OH1," Appl. Phys. Lett. **105**, 141115 (2014).
7. B. Dolasinski, P. E. Powers, J. W. Haus, and A. Coone, "Tunable narrow band difference frequency THz wave generation in DAST via dual seed PPLN OPG," Opt. Express **23**, 3669-3680 (2015).
8. K. Saito, T. Tanabe, and Y. Oyama, "Design of a GaP/Si composite waveguide for CW terahertz wave generation via difference frequency mixing," Appl. Opt. **53**, 3587-3592 (2014).
9. P. Liu, D. Xu, H. Yu, H. Zhang, Z. Li, K. Zhong, Y. Wang, and J. Yao, "Coupled-mode theory for Cherenkov-type guided-wave terahertz generation via cascaded difference frequency generation," J. Lightwave Technol. **31**, 2508-2514 (2013).
10. A. J. Lee and H. M. Pask, "Cascaded stimulated polariton scattering in a Mg:$LiNbO_3$ terahertz laser," Opt. Express **23**, 8687-8698 (2015).
11. K. Saito, T. Tanabe, and Y. Oyama, "Cascaded terahertz-wave generation efficiency in excess of the Manley-Rowe limit using a cavity phase-matched optical parametric oscillator," J. Opt. Soc. Am. B **32**, 617-621 (2015).
12. F. C. Zumsteg, J. D. Bierlein, and T. E. Gier, "$K_xRb_{1-x}TiOPO_4$: a new nonlinear optical material," J. Appl. Phys. **47**, 4980-4985 (1976).
13. I. Shoji, T. Kondo, A. Kitamoto, M. Shirane, and R. Ito, "Absolute scale of second-order nonlinear-optical coefficients," J. Opt. Soc. Am. B **14**, 2268-2294 (1997).
14. A. Hildenbrand, F. R. Wagner, H. Akhouayri, J. Y. Natoli, M. Commandré, F. Théodore, and H. Albrecht, "Laser-induced damage investigation at 1064 nm in $KTiOPO_4$ crystals and its analogy with $RbTiOPO_4$," Appl. Opt. **48**, 4263-4269 (2009).
15. H. Jang, G. Strömqvist, V. Pasiskevicius, and C. Canalias, "Control of forward stimulated polariton scattering in periodically-poled KTP crystals," Opt. Express **21**, 27277-27283 (2013).
16. W. Wang, Z. Cong, X. Chen, X. Zhang, Z. Qin, G. Tang, N. Li, C. Wang, and Q. Lu, "Terahertz parametric oscillator based on $KTiOPO_4$ crystal," Opt. Lett. **39**, 3706-3709 (2014).
17. T. Ortega, H. M. Pask, D. Spence, and A. Lee, "Competition effects between stimulated raman and polariton scattering in intracavity $KTiOPO_4$ crystal, "Advanced Solid State Lasers, Optical Society of America, **ATu3A**, ATu3A. 3 (2015).
18. L. Pálfalvi, J. Hebling, J. Kuhl, Á. Péter, and K. Polgár, "Temperature dependence of the absorption and refraction of Mg-doped congruent and stoichiometric $LiNbO_3$ in the THz range," J. Appl. Phys. **97**, 123505 (2005).
19. G. Kugel, F. Brehat, B. Wyncke, M. Fontana, G. Marnier, C. C. Nedelec, and J. Mangin, "The vibrational spectrum of a $KTiOPO_4$ single crystal studied by Raman and infrared reflectivity spectroscopy," J. Phys. C **21**, 5565-5583 (1988).
20. K. Kato and E. Takaoka, "Sellmeier and thermo-optic dispersion formulas for KTP," Appl. Opt. **41**, 5040-5044 (2012).
21. C. F. Hu, K. Zhong, J. L. Mei, M. R. Wang, S. B. Guo, W. Z. Xu, P. X. Liu, D. G. Xu, Y. Y. Wang, and J. Q. Yao, "Theoretical analysis of terahertz generation in periodically inverted nonlinear crystals based on cascaded difference frequency generation process," Mod. Phys. Lett. B **29**, 1450263 (2015).